Journal of Cleaner Production 319 (2021) 128582

Contents lists available at ScienceDirect

Journal of Cleaner Production

journal homepage: www.elsevier.com/locate/jclepro

A two-stage stochastic model for co-firing biomass supply chain networks

Maria Aranguren, Krystel K. Castillo-Villar *, Mario Aboytes-Ojeda

Mechanical Engineering Department and Texas Sustainable Energy Research Institute, University of Texas at San Antonio, One UTSA Circle, San Antonio, TX, USA

ARTICLE INFO

Handling Editor: M.T. Moreira

Keywords:
Optimization
Stochastic programming
Hub-and-spoke
Biomass
Supply chain
Metaheuristic
Simulated annealing

ABSTRACT

A sustainable alternative to fossil fuels is biomass. The design of cost-efficient biomass networks is necessary to compete with nonrenewable resources. The creation of integrated biomass supply chain (BSC) network design models and solution procedures can contribute to the achievement of this goal. In particular, the emerging bioenergy industry must take advantage of the economies of scale in transportation to minimize the final product's cost. Hub-and-spoke networks have been proposed as a modeling approach to design large scale BSCs. The majority of these models are deterministic and do not consider the inherent variability in the biomass feedstock, such as physical and chemical properties that affect transportation, the effects of future climate on the biomass supply, overall cost, and production operations. Levels of ash and moisture are directly related to the quality of the feedstock, which negatively affects production of biofuels, increasing transportation and handling costs as well as the burden on the BSC's efficiency. Varying weather affects biomass yield, which creates a fluctuation in the incoming supply into the network, creating a complex large scale Newsvendors Problem. In this paper, a stochastic hub-and-spoke network model and an efficient solution are proposed to minimize logistical costs by finding an optimal production and distribution network as well as optimal transportation while reducing computational burden by using metaheuristics, such as Simulated Annealing, when solving large NP-hard instances. The proposed solution procedure was compared to recent benchmark models, i.e. Bender's Decomposition, yielding an overall solution difference of less than 7.71% and average reduction time difference of 91.4%. Case studies with several scenarios based on varying weather conditions were created using realistic data from the northeast region of the U.S.

1. Introduction

In the United States, 30% of power generation stems from coal-fired power plants (U.S. Energy Information Administration, 2017). Several methods exist to mitigate Greenhouse Gas (GHG) emissions generated by these power plants. One method that has increased in popularity in recent years due to the growing interest in renewable energy is biomass co-firing. Co-firing entails replacing a fraction of the coal in the power plant with biomass. Due to biomass' zero net emission combustion, co-firing leads to a reduction in GHG emissions. Biomass co-firing may be done without altering the power plant's infrastructure if the replacement ratio remains below 20% (Tillman, 2000) to maintain the thermal efficiency. The implementation of biomass co-firing offers multiple benefits to the local economy. Aside from the reduction of GHG emission, the creation of transportation and agricultural jobs may help boost the local economy, which, in turn, nourishes the penetration of renewable energy into the power grid.

In reviewing recent works and analyses on biomass feedstock and bioenergy production, a similar theme constantly emerges: The main drivers in making biomass a viable sustainable energy source are transportation cost and supply chain practices (Liu et al., 2016). Additionally, biomass supply continuous to vary as the global climate changes (Daioglou et al., 2019). Therefore, minimizing the investment of procuring feedstock has been a key driver in biomass supply chain (BSC) design models. Similarly, we aim to minimize the cost associated with the BSC for co-firing purposes, which include harvesting and production activities as well as handling and transportation. To accomplish the aforementioned goal, we propose a two-stage stochastic hub-and-spoke model. Hub-and-spoke models have been presented in the literature as a promising method to optimize large scale BSC (Roni et al., 2014). Hub-and-spoke networks are also known to drastically increase in complexity with the size of the problem, which indicates a *NP-hard* behavior (Eiselt and Marianov, 2009). Therefore, exploring alternative solution procedures, such as metaheuristics, is a promising endeavor to decrease computational burden.

The contributions of our work involve modeling, methodology, and application. The *model* presented is a two-stage stochastic hub-and-spoke model for biomass co-firing in coal-fired power plants that integrates weather, as per biomass supply uncertainty, and biomass

* Corresponding author.
E-mail address: krystel.castillo@utsa.edu (K.K. Castillo-Villar).

https://doi.org/10.1016/j.jclepro.2021.128582
Received 28 September 2020; Received in revised form 16 July 2021; Accepted 5 August 2021
Available online 12 August 2021
0959-6526/© 2021 Elsevier Ltd. All rights reserved.

quality. Biomass supply stochasticity increases the complexity of the supply chain, leading to a more holistic solution as compared to previous studies. Additionally, integrating biomass quality hinders the efficiency of the supply chain, since moisture and ash incorporate additional cost and required supply to meet demand. Additionally, the BSC is optimized to minimize the cost associated with the procurement of biomass feedstock. Regarding *methodology*, we propose a hybrid solution procedure employing a tailored-made Simulated Annealing (SA) metaheuristic and the Simplex Method (SM). We compare its performance against benchmark methods, such as Bender's Decomposition (BD). Finally, the model and metaheuristics were to a realistic case study in the Northeastern Region of the United States, where the SA is tuned and tested. Through our research, we wish to determine how supply variability and biomass quality affect the BSC design for co-firing, and how to tackle large-scale instances where generic methods may not be enough. In consecutive sections, we present a detailed explanation of the proposed approach: Section 2 briefly discusses comparable previous works and places our study's contributions in context of recent research; Section 3 presents the mathematical formulation of the two-stage hub-and-spoke stochastic model, and Section 4 outlines the solution procedure through the presented SA metaheuristic; Section 5 outlines the case study including cost figures, assumptions, and scenario creation; Section 6 presents the numerical experimentation and the algorithm performance comparison; Section 7 elaborates on concluding remarks, managerial insights and future work.

2. Literature review

This section summarizes previous works in the literature, exclusively works focused on the optimization of BSCs applied to biomass co-firing in coal-fired power plants. Comprehensive literature reviews regarding BSC design and its inherent challenges and opportunities are outlined in the works of Ba et al. (2016), Lautala et al. (2015), Ghaderi et al. (2016), and Zand Atashbar et al. (2018). These reviews consider BSCs in a more general sense without focusing on a single application. More generally, these studies focus on biomass for the production of biofuels. Regardless, the fact remains that the most critical characteristics of a BSC design are transportation costs and activities associated with it, such as handling and delivery method. Specifically, Lautala et al. (2015) pointed out how many models lack consideration of environmental impact when designing their BSC models. Additionally, Ba et al. (2016) and Zand Atashbar et al. (2018) mentioned the lack of granularity in supply chains, especially when considering biomass production and harvesting. Additionally, Ba et al. (2016) mentioned the need to utilize open-source programs to facilitate dissemination. Finally, Ghaderi et al. (2016) noted that only 21.5% of the models they reviewed were nondeterministic, indicating the lack of sufficient research in this area. From a bioethanol perspective, multiple works have considered biomass quality as a worthy endeavor when designing an efficient BSC, as it often disrupts the SC and the biomass to bioethanol conversion process (Aboytes-Ojeda et al., 2019; Nur et al., 2020). Initial integration of supply uncertainty has also been considered leading the promising solutions and potential benefits for the development of biomass supply chains for co-firing (Mirkouei et al., 2017). Moreover, in the endeavor to explore alternative solution procedures regarding scalability and metaheuristic solution procedures for large scale instances, Aboytes-Ojeda et al. (2020) proposed a hybrid metaheuristic approach to reduce cost of the bioethanol supply chain, showing promising results from the integration of a hybrid Simulated Annealing (SA) solution procedure, leaving room for further development and research for the application of such metaheuristics for biomass production and supply chain design for co-firing purposes. Noteworthy is that these works provide a great summary of the challenges faced while optimizing a BSC. They additionally do an excellent job at recognizing various optimization methods, but they do not necessarily focus on biomass co-firing at coal power plants. As a consensus, all of these works agree that biomass logistics must be continuously improved to make bioenergy a competitive means of renewable energy production.

After considering the broader BSC analyses seen in the literature, we would like to focus specifically on works in which a BSC is designed for the purposes of co-firing at coal-fired power plants. To begin with, Roni et al. (2014) presented a hub-and-spoke model, in which long-haul transportation of large quantities of biomass was considered, since the proposed BSC covered a large portion of the United States. Roni et al. (2014) extended the hub-and-spoke design by integrating a step-wide cost function for the transportation cost. Furthermore, Roni et al. concluded that biomass within a 75-mile radius had a transportation cost of $8.53/dry ton and that any biomass not located within this radius was no longer economically viable to use for co-firing. Furthermore, similar results can be seen in the work of Kizha et al. (2015); their case study in northern California conducting woody biomass procurement showed how proximity of feedstock to the power plant aids in making the biomass in question more economically competitive when compared to other suppliers. Kizha et al. (2015) also consider competition within the BSC and concluded that it may be augmented through an increase of biomass consumers in the market. Noteworthy, Roni et al. (2014) and Kizha et al. (2015) concluded that the closer the biomass supply is to the power plant, the more economically competitive biomass co-firing becomes. Therefore, analyzing a BSC that produces and harvests biomass close to coal-fired power plants is a suitable strategy.

Regarding stochastic models, Poudel et al. (2016) considered a two-stage stochastic model to manage a BSC. Feedstock supply uncertainty was analyzed in this model considering: season-wide utilization of multimodel facilities, number of containers for transportation purposes, and the quantity of biomass to be processed, stored, and delivered. The case study presented by Poudel et al. (2016) took place in various counties in the states of Mississippi and Alabama. Their conclusions indicated that high variability within the biomass feedstock increased transportation costs by $1.87/ton. The BSC presented by Poudel et al. (2016) determined feedstock variability considering historical data as the main driver. Further research on methods to better understand biomass production and harvesting is required, especially research considering feedstock variability under future climate prediction models to create more realistic scenarios. Additionally, Poudel et al. (2016) noted the fact that solving a stochastic model creates a large computational burden. To overcome such challenges, they integrated a prediction methodology for the biomass feedstock. Therefore, analyzing further solution methodologies that may lower computational burden in the design of BSCs is sought after in the literature, especially as problems increase in size, granularity and uncertainty.

Considering the long-haul transportation of biomass, the work De Laporte et al. (2016) analyzed BSCs by taking into account the use of rail transportation and biomass exportation. Laporte et al. (2016), two power plants were analyzed along with international exports, considering pellets and bales as formats for biomass delivery. Laporte et al. (2016) concluded that the local transportation model was superior to the exportation of biomass, indicating that local BSCs are more efficient and economically competitive than their long-haul counterparts. Therefore, local production of biomass is preferable to long-haul models, and recreating realistic locally-sourced BSCs would yield beneficial to its over efficiency and cost reduction.

After analyzing the literature for the design and analysis of BSCs for co-firing, the focus was switched to a smaller niche, where BSCs were designed at a more local level to consider farm level feedstock production as part of the optimization model. First, the work by Hart et al. (2016) proposed a Mixed Integer Linear Programming (MILP) model and tested it on a realistic case study in the Texas region. Hart et al. (2016) considered feedstock supply in hand-picked farm areas through the use of the *Agricultural Land Management Alternative with Numerical Assessment Criteria* (ALMANAC) without much detail or granularity on the farm selection process. Furthermore, Hart et al.

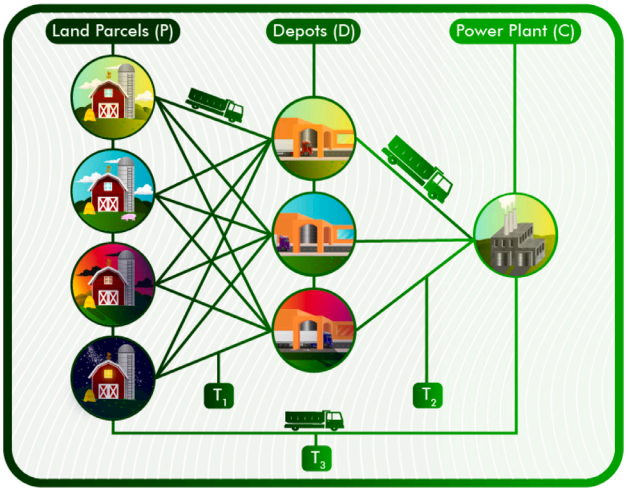

Fig. 1. Supply Chain Network Presentation (Aranguren et al., 2018).

(2016) considered historical weather data in a single scenario. Harts's work motivated the work of Aranguren et al. (2018), which increased the granularity of the biomass supply estimation by simulating the supply in planting locations (parcels) with a 100-hectare resolution (over 5000 parcels), considering soil type, potential yield, and historical and future climate scenarios. However, their work was deterministic and yielded various supply chain designs for each climate scenario. This is not particularly useful since it is uncertain which scenario will occur in the future and which BSC design is the most convenient. This limitation can be resolved by implementing an stochastic model, which yields a single BSC design considering all future climate scenarios.

The related works that were discussed exhibit the inspiration and the basis for the work presented here. In this paper, we extend and complement previous efforts by proposing a two-stage stochastic hub-and-spoke model, considering biomass quality, future climate impact on biomass supply, local environmental impact, and a farm-level feedstock simulation through the United States Department of Agriculture(USDA)'s simulation software ALMANAC, and we finally present a tailor-made metaheuristic to solve large scale instances of the supply chain while decreasing computational burden (see Table 1).

3. Mathematical formulation

This section presents the mathematical formulation for the two-stage stochastic hub-and-spoke model. As seen in Fig. 1, the logistics network entails three sets of arcs. The first-stage variables entail the selection of depot locations, W_i, and therefore an investment decision in supply chain design. Additionally, the second stage variables are affected by stochastic weather scenarios, o, which impact required biomass supply availability and logistics. Hence, the second-stage stochastic variables are related to biomass yield, which include: $X_{ij}(o)$, $Y_{jk}(o)$, $Z_{ik}(o)$, and $\pi(o)$.

Decision variables:

- W_j: binary variable - 1 if $j \in D$ is used, and 0 otherwise
- $X_{ij}(o)$: flow along arc $(i,j) \in T_1$ from parcel (P) to depot facility (D)
- $Y_{jk}(o)$: flow along arc $(j,k) \in T_2$ from depot facility (D) to coal power plant (C)
- $Z_{ik}(o)$: flow along arc $(i,k) \in T_3$ from parcel (P) to coal power plant (C)
- $\pi(o)$: third-party biomass supply

Parameters:

- $c_{ij}^{T_1}$: cost charged per metric ton shipped along $(i,j) \in T_1$
- $c_{jk}^{T_2}$: cost charged per metric ton shipped along $(j,k) \in T_2$
- $c_{ik}^{T_3}$: cost charged per metric ton shipped along $(i,k) \in T_3$
- ξ_j: fixed investment cost to install a depot at node $j \in D$
- ζ: cost per metric ton of biomass from third-party
- $p(o)$: scenario probability for $o \in \Omega$
- u_j: storage capacity of depot facility $j \in D$
- m_i: moisture level of biomass supply from parcel $i \in P$
- s_i: supply of biomass at parcel location $i \in P$
- d_k: biomass demand at coal power plant $k \in C$

$$Min: \sum_{j\in D} \xi_j W_j + \sum_{o\in\Omega} p(o)[\sum_{i\in P}\sum_{j\in D} c_{ij}^{T_1} X_{ij}(o) + \sum_{j\in D}\sum_{k\in C} c_{jk}^{T_2} Y_{jk}(o) + \sum_{i\in P}\sum_{k\in C} c_{ik}^{T_3} Z_{ik}(o) + \zeta\pi(o)] \quad (1)$$

Subject to:

$$\sum_{j\in D} X_{ij}(o) + \sum_{k\in C} Z_{ik}(o) \le s_i(o) \quad \forall i \in P \quad o \in \Omega \quad (2)$$

$$\sum_{i\in P}(1-m_i)X_{ij}(o) = \sum_{k\in C} Y_{jk}(o) \quad \forall j \in D \quad o \in \Omega \quad (3)$$

$$\sum_{i\in P} X_{ij}(o) \le u_j W_j \quad \forall j \in D \quad o \in \Omega \quad (4)$$

$$\sum_{j\in D} Y_{jk}(o) + \sum_{i\in P}(1-m_i)Z_{ik}(o) + \pi(o) = d_k \quad \forall k \in C \quad o \in \Omega \quad (5)$$

$$(i,j) \in T_1 \quad (j,k) \in T_2 \quad (i,k) \in T_3 \quad (6)$$

$$X_{ij}(o), Y_{jk}(o), Z_{ik}(o), \pi(o) \in R^+ \quad o \in \Omega \quad (7)$$

$$W_j \in \{0,1\} \quad \forall j \in D \quad (8)$$

The objective function (1) is to minimize the expected cost for harvesting, processing, and transporting switchgrass as well as depot investment costs. Constraints (2) restrict the supply from the parcels to the maximum yield, (3) assure a mass balance in depots and (4) limit depot storage capacity. The demand of each power plant is satisfied due to constraints (5). Constraints (6) set arc definitions, and constraints (7) assure a non-negative flow in arcs. Constraints (8) set the binary limitations for depot selection variables.

4. Solution procedure

Due to the nature of hub-and-spoke networks, the problem at hand is considered *NP-hard* (Eiselt and Marianov, 2009), which makes the use of metaheuristics a feasible alternative to solving said model with a reasonable computational burden. In this paper, we propose a Simulated Annealing (SA)-based approach to solve a realistic instance in the Northeast Region of the United States. To accomplish this, the metaheuristic is tailored to take advantage of the nature of the hub-and-spoke network. The SA algorithm is inspired by the physical process of heating a metal and subsequently, rapidly lowering its temperature to alter its molecular structure, thereby decreasing defects and minimizing the system's energy (Siarry, 2016).

The initial solution for the system's energy begins with the entirety of the biomass demand being met by a third party, which entails a large penalty cost of $100 due to the inability to meet the demand through the designed BSC (U.S. Department of Energy, 2016). The solution topology is analyzed through neighborhood moves; these consist of adding, removing or swapping potential depot locations (refer to Section 5.6 for more details). A simplified representation of neighborhood moves may be seen in Fig. 3. With swapping, the temperature influences the neighborhood move: At the start of the algorithm, when the temperature is high, a higher range of depot selection is promoted,

Table 1
Literature review in co-firing biomass supply chain optimization models.

Reference	Model	Solution procedure	Type	Climate considerations	Biomass quality	Large scale approach
Roni et al. (2014)	Hub-and-Spoke MILP	Benders Decomposition	D	○	○	○
Kizha et al. (2015)	Qualitative Biomass Competition Model	Economic Approach	D	○	○	○
Poudel et al. (2016)	Two-stage Stochastic	Hybrid Decomposition Algorithm	S	○	○	⊘
Laporte et al. (2016)	NPV Maximization Model	GIS/Economic Approach	D	⊘	○	○
Hart et al. (2016)	Hub-and-Spoke MILP	Simplex	D	○	○	○
Aranguren et al. (2018)	Hub-and-Spoke MILP	Simplex	D	⊘	○	○
This article	Hub-and-Spoke Two-stage Stochastic	SA Metaheuristic	S	⊘	⊘	⊘

D - Deterministic; S - Stochastic.

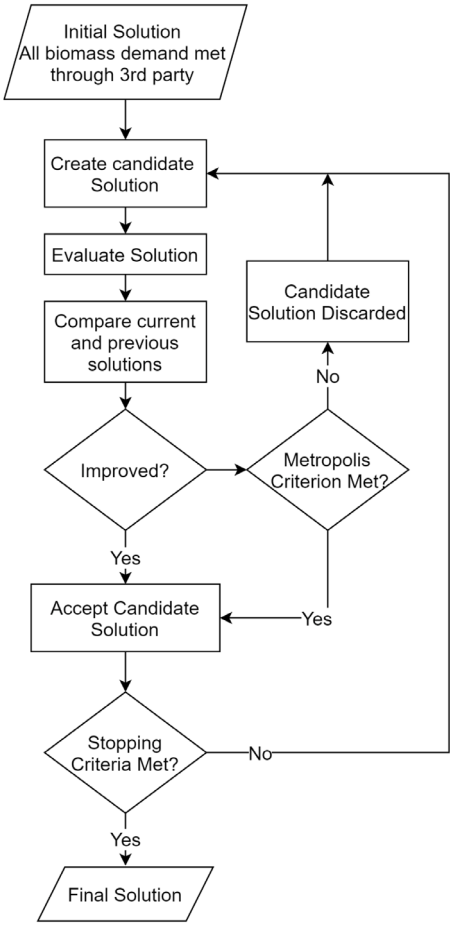

Fig. 2. Simulated Annealing General Algorithm.

thus, allowing for a more aggressive exploration of the topologies of the logistic network. In contrast, towards the end of the optimization process, when the temperature has decreased, less depots are interchanged. The neighborhood moves of adding and removing are chosen at random and depend on the currently selected locations: As more potential depots are selected, the higher the likelihood for removal is, and the opposite is true for adding. The generic SA algorithm is summarized in Fig. 2, and the tailored, more detailed, pseudo code is displayed in Table 2.

Simulated annealing metaheuristic notation:

- D: Total number of potential depots
- Q_1: BSC Model
- $E_0 = c_0$: Initial energy as related to the cost of the initial solution

Table 2
Simulated annealing metaheuristics tailored solution procedure.

- ▷ START
- ▷ Generate data structures. $W^* = W_{base} = \varnothing$
- ▷ Obtain initial solution for model Q_1, 3rd party cost: $E^* = E_0 = c_0$
  - ■ FOR $T = T_{max} : T_{min}$
    - ∘ Random integer generation: $r_w \in [0, Df]$
    - ∘ Calculate $\Delta W_i = r_w - N_{W_{base}}$
    - ∘ IF $\Delta W_i > 0$
      - • FOR $j = 1 : \Delta W_i$
        - ◇ Random location added: $W_r = 1$ in W_{base}
    - ∘ ELSEIF $\Delta W_i < 0$
      - • FOR $j = 1 : \Delta W_i$
        - ◇ Random location removed: $W_r = 0$ in W_{base}
    - ∘ ELSEIF $\Delta W_i = 0$
      - • Random integer generation: r_{w_1}, $r_{w_2} \in [0, Df]$
      - • FOR $j = 1 : T$
        - ◇ Depot status swapped: $W_{r_{w_1}}, W_{r_{w_0}} \in W_{base}$
    - ∘ Set first-stage variables and obtain second-stage variables solving with SM (i.e., find E_i)
    - ∘ Calculate the change in energy $\Delta E_i = E^* - E_i$
    - ∘ IF $\Delta E_i > 0$
      - ◇ Select E_i
      - ◇ Set $E^* = E_i$
      - ◇ Update solution, data structures
    - ∘ ELSEIF $e^{\Delta E_i/T} > r$
      - ◇ Select E_i
      - ◇ Update solution, data structures
    - ∘ ELSE
      - ◇ Discard solution. No change to data structures
- ▷ END

- E_*: Current best solution
- E_i: Energy at iteration i
- T_i: Temperature at iteration i
- T_{max}: Maximum initial temperature
- T_{min}: Minimum final temperature
- f: Potential depot search factor
- $W^* = W_{base}$: Depot selection data structure base
- N_{W_base}: Number of depots selected in base
- W_i: Depot selected at iteration i
- W_r: Randomly selected depot location
- SM: Simplex Method
- r_w: Randomly generated number

Further analysis of algorithm parameters is required for optimal performance. Initial temperature and search factor are tuned through a factorial experimental design. Initial temperature of the model affects the rate of *swapping* neighborhood moves and the *Metropolis* acceptance criterion. The Metropolis criterion entails accepting a non-improving solution under certain circumstances: In the presented SA, a non-improving solution (i.e., $\Delta E_i < 0$) will be accepted if $e^{\Delta E_i/T}$ is greater than r, a randomly generated number. The higher the temperature, the more likely non-improving moves will be accepted. However, if the initial temperature is not high enough, none of these neighborhood moves will be accepted, leading to little exploration of the topology as

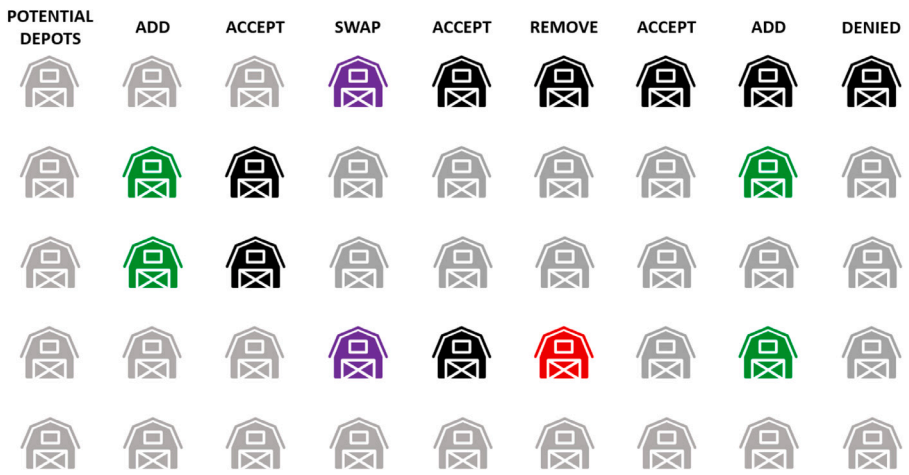

Fig. 3. Simulated Annealing Neighborhood Move in Detail.

well as the possibility of remaining in a local optimum. Additionally, the search factor (f) affects the random selection of depots and exploration; therefore, it should be examined, as it affects solution time. Fig. 4 shows the outcome of the design of experiments to tune these SA parameters. Here, we determine that a starting temperature of 1000 is reasonable, as it yields consistent results for the Best Solution (BS) when compared to 2000 and 3000. Furthermore, with regard to the search factor, 20% shows more promise, as it allows for greater exploration of the topology while remaining competitive against the benchmark, Bender's Decomposition.

5. Case study

The proposed case study considers the work of Aguilar et al. (2012) as a baseline for the locations selected for BSC. Aguilar et al. (2012) analyzed biomass co-firing potential in the northeastern region of the U.S. Specific variables were examined to determine the optimal county locations for biomass co-firing: St. Louis, MN; Delta, MI; Dane, WI; Schuylkill, PA; Marshall, WV; Woodbury, IA; Monroe, NY; Grant, WI; Brown, WI. For the BSC in our case study, active coal-power plants were selected from these counties as determined by the 2016 eGrid (U.S. Environmental Protection Agency, 2016) (see Fig. 5).

5.1. Potential biomass yield through ALMANAC

Using USDA's Soil Survey Geographic Database (SSURGO) (U.S. Department of Agriculture Web Soil Survey, 2017) and ArcMap mapping capabilities (esri, 2020), a raster of 1/16 decimal degrees (dd) resolution was created to divide the selected areas. These coordinates were then used as inputs to determine the potential yield of the parcels using the Agricultural Land Management with Numerical Assessment Criteria (ALMANAC) simulation model (Kiniry et al., 1996). Additionally, the National Land Cover Database (Anon, 2017) was used to circumvent locations which may negatively affect the environment and/or are unrealistic, such as forested and developed areas.

Similar to the work of Hart et al. (2016) in Texas, the highest yielding biomass for the area must be determined. For the area in question, a 100-mile radius around each coal-power plant was considered as a potential biomass supply, and 100 parcels were randomly selected to simulate biomass growth through ALMANAC for commonly known biomass types. The results are shown in Table 3.

Noteworthy is that ALMANAC does not have built-in capabilities for Miscanthus simulation. Therefore, with the aid of experimental databases from the Idaho National Lab (Idaho National Lab, 2019) and ALMANAC experts from USDA, ALMANAC was calibrated to output realistic Miscanthus yields for the case study area. Due to similarities in the behavior of Miscanthus and Switchgrass, a t-test was conducted to determine if their difference was statistically significant: With a confidence level of 95%, the t-test indicated a nonsignificant difference between the yields with regard to the raw data in tons/ha. However, once converted to MBtu/ton, the t-test yielded a significant difference with a p-value of 0.0006897. Therefore, Miscanthus was used in the BSC design due to its high yield density and net caloric value.

Table 3
Average yields of common biomass types.

	Corn	Sorghum	Wheat	Switchgrass	Miscanthus
Avg. Yield[a]	6.623	4.249	0.654	13.45	13.63
Net Caloric Value[b]	14.58	14.45	13.96	14.88	15.59
Avg. Yield[c]	96.58	61.39	9.135	200.2	212.5

[a]ton/hectare.
[b]MMBtu/ton.
[c]MMBtu/hectare.

Table 4
Biomass demand by power plant.

Power Plants	20% Coal[a]	Coal to MMBtu	Miscanthus[a]
1	176,604	3,898,313	250,000
2	248,914	5,494,472	352,362
3	67,652	1,493,341	95,768
4	74,410	1,642,519	105,335
5	19,760	436,186	27,973
6	94,396	208,3681	133,627
7	40,668	897,717	57,571
8	8324	183,741	11,783
9	31,623	698,034	44,765
10	27,688	611,176	39,195
11	706,545	15,596,103	1,000,181

[a]tons.

5.2. Biomass demand

A total of 11 coal-power plants were selected after considering the work of Aguilar et al. (2012) and the current active facilities (U.S. Environmental Protection Agency, 2016). The required demand of each power plant at a 20% co-firing rate is shown in Table 4. Noteworthy, as seen in Table 4, the energy ratio of the coal to biomass was considered to obtain the Miscanthus dry mass required to meet the energy requirements of the 20% of coal being replaced.

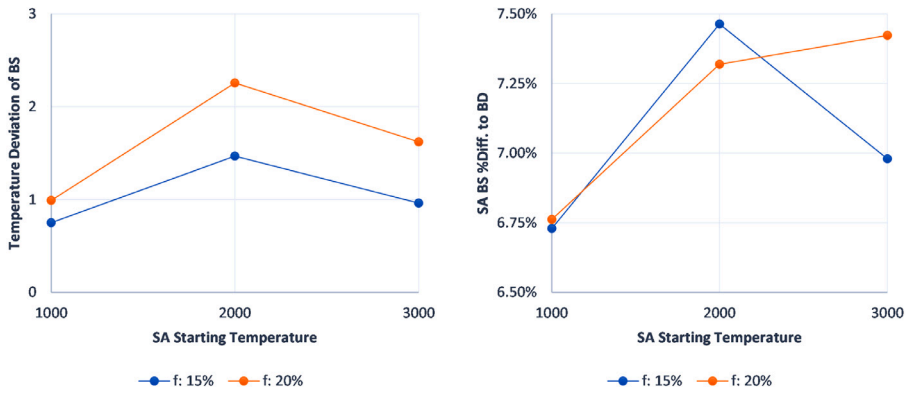

Fig. 4. Experimental Analysis of SA Tuning Parameters.

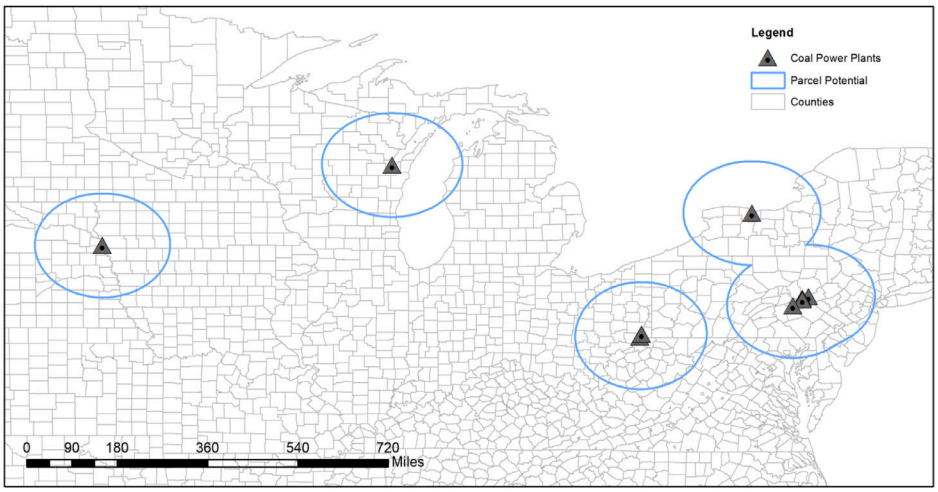

Fig. 5. BSC Design — Area of Study: 11 Coal-power plants, 100-mile radius of potential farm land for each.

Table 5
Cost per harvesting activity (Larson et al., 2010).

Harvesting activity	Cost
Swathing (σ)	$32.49/hectare
Fertilization (γ)	$10.23/hectare
Bailing (β)	$12.42/ton

Table 6
Cost per transportation activity (Griffith et al., 2010).

Transportation activity	Cost
Average truck speed (v)	60 km/hr
Truck operational cost (ω)	$48.40/hr
Small truck capacity (ρ^{T_1}, ρ^{T_3})	3.63 tons
Large truck capacity (ρ^{T_2})	21.76 tons
Loading (L)	$3.59/ton
Unloading (U)	$3.58/ton
Stacking (μ)	$0.44/ton

5.3. Farming and transportation costs

The costs related to the depot investment, harvesting, collection, and transportation of biomass were obtained through the work of Aranguren et al. (2018). However, the costs related to the rent of nonirrigated agricultural land was obtained from a nationwide analysis by the USDA from 2017 for each county in consideration (U.S. Department of Agriculture, 2017). Additionally, the cost associated with ash disposal content was also included in the transportation cost to account for biomass quality and its effect on the BSC total investment cost, see Section 5.4 for more information.

$$\phi_i = \beta + \frac{\gamma + \sigma + R_i}{s_i} \tag{9}$$

Where ϕ_i represents the total harvesting cost for parcel i, including the rent R for the specified parcel i depending on its county location (U.S. Department of Agriculture, 2017), and the biomass supply s from parcel i obtained from the ALMANAC simulation. Additional harvesting activity cost shown in Table 5.

$$\tau_{ij}^{T_1} = L + U + \mu + \frac{\frac{x_{ij}}{v}\omega}{\rho^{T_1}} \tag{10}$$

$$\tau_{jk}^{T_2} = L + U + \mu + \frac{\frac{x_{jk}}{v}\omega}{\rho^{T_2}} \tag{11}$$

$$\tau_{ik}^{T_3} = L + U + \mu + \frac{\frac{x_{ik}}{v}\omega}{\rho^{T_3}} \tag{12}$$

Where τ refers to the transportation cost in each arc of the supply chain: T_1 from Parcel i to Depot j, T_2 from Depot j to Plant k, and T_3 from Parcel i to Plant k. Each τ considers the distance x associated with each arc. The distances used for x are obtained through the shortest route algorithm from the Open Source Routing Machine (OSRM) platform (OSRM, 2017). Additional transportation costs associated with each τ are shown in Table 6. The total cost per ton of biomass is then

obtained with the combination of the previous equations:

$$c_{ij}^{T_1} = \phi_i + \tau_{ij}^{T_1} \quad c_{ik}^{T_3} = \phi_i + \tau_{ik}^{T_3} \quad c_{jk}^{T_2} = \tau_{jk}^{T_2} \tag{13}$$

5.4. Biomass quality

As seen in the literature, biomass quality is able to influence BSC design. Features such as moisture and ash can increase the cost of procuring biomass. The demand for biomass by coal-fired power plants is considered dry biomass. Wet bulk density, ρ_b, is related to dry bulk density, ρ_d, and moisture content, M_w as shown in (14) (Aboytes-Ojeda et al., 2019).

$$\rho_b = \rho_d(1 + M_w) \tag{14}$$

Therefore, in order to meet the demand presented by the coal-fired power plants, the required biomass in the BSC must be greater to offset the moisture content penalty. Furthermore, if third-party biomass is required to meet the demand, the supply will be assumed to be dry, with a penalty cost of $100 per metric ton (U.S. Department of Energy, 2016). Moisture in the Miscanthus was derived from field sample data from the INL database (Idaho National Lab, 2019). However, the field sample data shows that the moisture is higher towards the coastal areas and lower towards the center of the U.S. To obtain moisture values for the rest of the locations, a linear regression was conducted to relate the planting location and the crop's moisture ($R^2 = 0.915/P - value < 0.0001$). Furthermore, normally distributed values were obtained for each location in combination with the results from the linear regression. The output from the resulting moisture analysis can be seen in Fig. 6.

Ash is another biomass characteristic shown in various BSC design studies that entails economic drawbacks. However, when considered in a BSC design leading to co-firing at coal power plants, there is no information in the literature at this time that outlines drawbacks to the power plant (Jaap and Sjaak, 2008). However, considering ash before it is delivered at the coal-power plant, ash may have a negative effect in the BSC design: due to disposal of ash residue. Discarding ash properly entails an additional cost in the supply chain: Waste disposal costs $28.86 per metric ton (Kenney et al., 2013). To determine Miscanthus' ash contents in the region, sample data from the Idaho National Labs (INL) was observed (Idaho National Lab, 2019). Given the locations available in the data set, small ash variation can be seen from place to place. Implementing a t-test between the locations in the INL ash data set yielded little difference in the samples, with a p-value of 0.13334 under a confidence of 0.05. Therefore, normally distributed random numbers were generated to simulate ash variation with a calculated mean of 1.4% and a standard deviation of 1% (Idaho National Lab, 2019).

5.5. Weather scenarios

To estimate the long-term impact of climate change, including drought and excess water periods, on crop yield, 25 years (2020 to 2045) of daily climate projections were obtained from the World Climate Research Programmes Coupled Model Inter-comparing Project Phase 5 (CMIP5) (Reclamation, 2013). The climate scenarios considered: the representative concentration pathway (RCP) 4.5. The RCP4.5 assumes that GHG emissions will peak at approximately 2040 and decrease after that year (van Vuuren et al., 2011). The data include precipitation and minimum and maximum temperature in a daily time step obtained for the center of each county of the spatial domain. A total of 287 Localized Constructed Analog (LOCA) time series were obtained. The names of the models and origin institutions are listed in Table 7. The weather scenarios obtained are then inputted into ALMANAC to obtain the simulated biomass supply for each parcel, where the scenarios in the proposed model have an uniform probability, and therefore, equality considered in the final solution.

Table 7
Origins of weather models.

Model	Agency
ACCESS1–0	ARC Centre of Excellence for Climate System Science Data Manager
ACCESS1–3	Research Data Australia
CCSM4	Community Earth System Model
CESM1-BGC	Community Earth System Model
CESM1-CAM5	Community Earth System Model
CMCC-CM	Centro Euro-Mediterraneo sui cambiamenti Climatici
CMCC-CMS	Centro Euro-Mediterraneo sui cambiamenti Climatici
CNRM-CM5	CNRM-GAME (Meteo-France/CNRS) and CERFACS since 1995
CSIRO-Mk3-6–0	The Centre for Australian Weather and Climate Research
CanESM2	Canadian Centre for Climate Modelling and Analysis
EC-EARTH	A European community Earth-System Model
FGOALS-g2	China National Committee for International Association of Meteorology and Atmospheric Sciences
GFDL-CM3	Geophysical Fluid Dynamics Laboratory
GFDL-ESM2G	Geophysical Fluid Dynamics Laboratory
GFDL-ESM2M	Geophysical Fluid Dynamics Laboratory
GISS-E2-H	NASA
GISS-E2-R	NASA
HadGEM2-AO	GeoScientific Model Development
HadGEM2-CC	GeoScientific Model Development
HadGEM2-ES	GeoScientific Model Development
IPSL-CM5A-LR	European Network for Earth System Modelling
IPSL-CM5A-MR	European Network for Earth System Modelling
MIROC-ESM	Japan Agency for Marine-Earth Science and Technology
MIROC-ESM-CHEM	Japan Agency for Marine-Earth Science and Technology
MIROC5	Atmosphere and Ocean Research Institute, The University of Tokyo
MPI-ESM-LR	Max-Planck-Institut Fur Meteorologie
MPI-ESM-MR	Max-Planck-Institut Fur Meteorologie
MRI-CGCM3	Meteorological Research Institute, Tsukuba, Japan
NorESM1-M	Institute for Meteorology and Climate Research, Karlsruhe Institute of Technology
bcc-csm1–1	Beijing Climate Center
bcc-csm1-1-m	Beijing Climate Center
inmcm4	Izvestiya, Atmospheric and Oceanic Physics

Table 8
Depot configuration from Heuristic.

▷ START
▷ Generate data structures: $\lambda_i = s_i / \sum_{o \in \Omega} p(o)(\sum_{i \in P} s_i)$; $D_{select} = \varnothing$
▷ Set hyper-parameters: α, β
■ FOR i in 1 : P
∘ FOR k in 1 : C
• If $x_{ik} \leq \beta$
◇ If $\lambda_i \leq \alpha$
Append to D_{select}
▷ END

5.6. Depot selection

Depots in hub-and-spoke networks are used as hubs to consolidate products in order to ship them in larger vessels, which often aids in improving the efficiency of the supply chain. The potential locations of the depots were obtained using the potential parcel locations. A heuristic was used that considers the parcel-plant (x_{ik}) distance and parcel yield (s_i). The yield was used to calculate a comparison factor, λ_i, to determine which parcels contribute the most to the overall supply. The distance limit, β, remained constant to consider all depots at 100 miles or less. The heuristic iterates through each power plant location, ensuring that each has a few potential depot locations around them. In the heuristic, the hyper-parameter α was altered to obtain various potential depot arrangements to test the SA algorithm's scalability, limiting the λ_i supply ratio to selected higher yielding areas to be selected as potential depot locations. A pseudo-code of the depot selection heuristic may be seen in Table 8, and an output of this heuristic is depicted in Fig. 7.

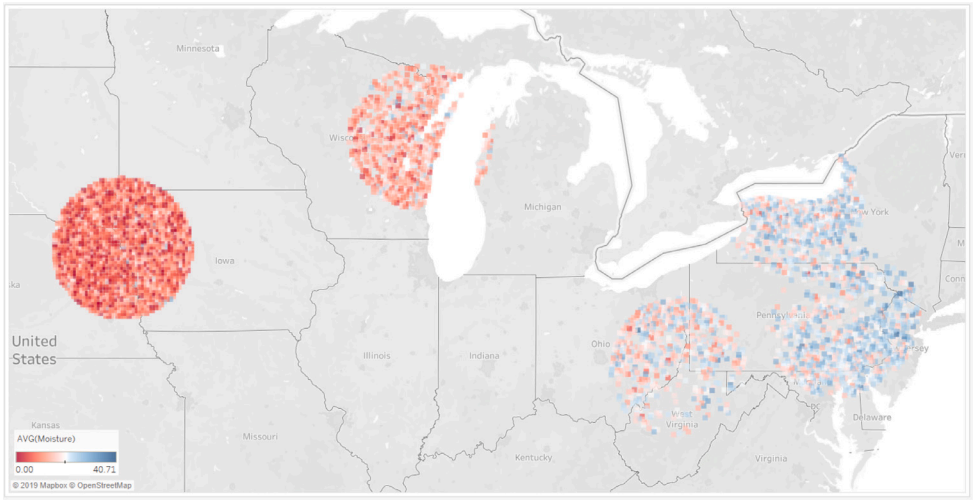

Fig. 6. Geographical Distribution of Moisture Percentages.

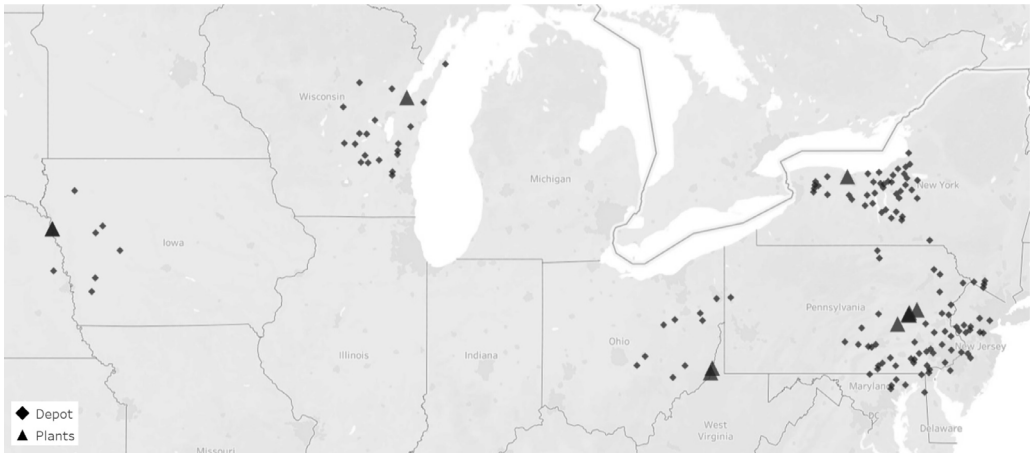

Fig. 7. Potential Depot Locations over Potential Biomass Yield; $\alpha = 0.2075$; $\beta = 100$.

6. Numerical analysis and results

The following section outlines the results of a sensitivity analysis showing how biomass quality affects the supply chain, in addition to the insight into the solutions obtained when the proposed solution procedure is applied to the presented case study for multiple experimental problem layouts.

The implementation of quality has implications in the planning and design of the BSC. Biomass quality, such as ash and moisture, impact the overall cost and topology of the supply chain. To determine the impact of biomass quality, two instances were considered: quality and non-quality (Table 9). It is noteworthy that the solutions differ in cost. The percent difference in overall investment of quality versus non-quality instances is 17%, with the transportation cost increasing by 19% and harvesting by 16%. The differences in cost show substantial consequences to the BSC design when considering biomass quality, and therefore, further emphasizes the need for its implementation.

The experiments were conducted in a workstation with an Intel(R) Cost (TM) i9-7980XE central processor unit operating at a frequency of 2.40 GHz and 32 GB of random-access memory. As shown in Table 12, as the size of the problem increases (defined in Table 10), the time required to find a solution also increases, which is expected for an *NP-hard* problem. Table 12 shows that, for small instances, Bender's Decomposition is able to solve the problem within minutes, but, as soon

Table 9
Investment comparison due to biomass quality in BSC.

	Non-Quality	Quality	% Diff.
Tot. harvest	2.119E+06 tons	2.511E+06 tons	16%
Harvesting cost	$5.615E+07	$6.673E+07	16%
Transportation cost	$3.363E+07	$4.147E+07	19%
Total investment	$9.278E+07	$1.112E+08	17%

Table 10
Summary of experimental problems.

ID	Variables				No. of variables			No. of constraints
	Plants	Depots	Parcels	Ω	Continuous	Binary	Total	
1	11	106	3,750	5	2,199,580	106	2,199,686	19,865
2	11	106	3750	10	4,399,160	106	4,399,266	39,730
3	11	106	3750	20	8,798,320	106	8,798,426	79,460
4	11	106	3750	31	13,637,396	106	13,637,502	123,163
5	11	202	3750	5	4,004,860	202	4,005,062	20,825
6	11	202	3750	10	8,009,720	202	8,009,922	41,650
7	11	202	3750	20	16,019,440	202	16,019,642	83,300
8	11	202	3750	31	24,830,132	202	24,830,334	129,115
9	11	295	3750	5	5,753,725	295	5,754,020	21,755
10	11	295	3750	10	11,507,450	295	11,507,745	43,510
11	11	295	3750	20	23,014,900	295	23,015,195	87,020
12	11	295	3750	31	35,673,095	295	35,673,390	134,881

Table 11
Breakdown cost comparison per Arc.

ID	BD Depots	BD T1 ($M)	BD T2 ($M)	BD T3 ($M)	SA Depots	SA T1 ($M)	SA T2 ($M)	SA T3 ($M)
1	6	48.9	6.50	58.4	3.8	52.0	6.94	62.3
2	6	48.8	6.50	58.4	5.2	51.8	6.87	61.8
3	6	48.9	6.50	58.4	6.2	51.3	6.81	61.2
4	7	56.9	7.68	48.9	7.4	59.9	8.11	51.7
5	8	62.9	7.72	40.1	7.2	67.5	8.34	43.4
6	8	63.2	7.75	39.8	8	67.0	8.15	41.8
7	8	63.3	7.78	39.6	8.4	67.8	8.34	42.5
8	8	63.5	7.79	39.5	6.4	68.7	8.38	42.5
9	9	72.0	9.17	27.0	11.2	76.6	9.83	29.0
10	9	72.1	9.19	26.9	9.6	77.3	9.86	28.9
11	9	72.1	9.19	26.9	13.4	76.5	9.76	28.6
12	9	72.1	9.19	26.9	10.2	76.4	9.77	28.6

BD: Bender's Decomposition — SA: Simulated Annealing — T1: P to D — T2: D to C — T3: P to C.

Table 12
Summary of experimental results.

ID	BD time (s)	SA BS time (s)	BD Sol ($M)	BD Gap	SA solution ($M)	Sol %Diff	Time %Diff
1	220.68	24.04	115.71	Standard	123.33	6.59%	89.10%
2	533.91	67.49	115.78	Standard	122.39	5.71%	87.36%
3	1922.25	120.25	115.81	Standard	121.60	5.01%	93.74%
4	2398.44	197.38	115.82	0.01%	122.02	5.35%	91.77%
5	1239.30	31.538	113.34	Standard	121.35	7.06%	97.46%
6	1502.88	106.32	113.38	Standard	120.27	6.08%	91.42%
7	3002.83	246.51	113.40	0.07%	121.48	7.13%	91.79%
8	3736.86	363.88	113.40	0.07%	122.14	7.71%	90.26%
9	905.72	102.23	111.19	Standard	118.65	6.71%	88.71%
10	2230.06	139.86	111.21	0.03%	119.55	7.50%	93.73%
11	3185.50	419.78	111.22	0.03%	118.18	6.25%	86.82%
12	13771.35	710.51	111.22	0.03%	118.08	6.17%	94.84%

BD: Bender's Decomposition — SA: Simulated Annealing — BS: Best Solution.

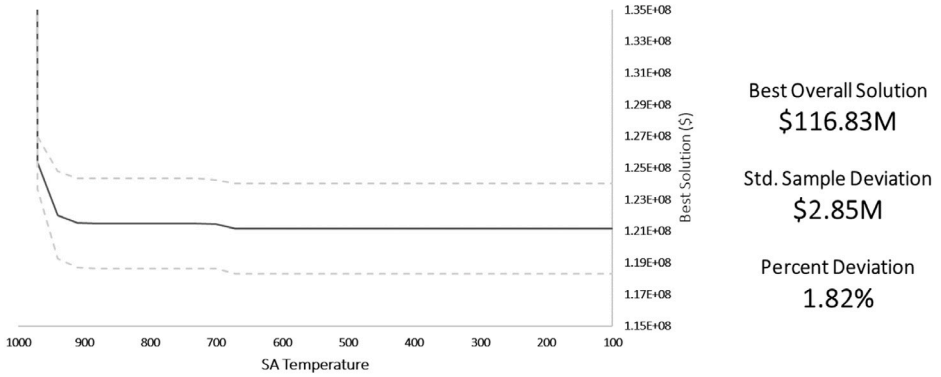

Fig. 8. Best Solution per SA Iteration.

as a threshold is reached, BD is unable to obtain a solution due to lack of memory, and the standard gap (1e-4) has to be slightly widened for some instances. By implementing the SA, larger instances are solved without the issue of memory limits, and it is considerably faster when compared to the benchmark, Bender's Decomposition. For the largest instance (#12), the difference in CPU time is 94.84%. For all instances, the solution percent difference between the two algorithms remains below 7.71% with an average time percent difference of 91.4%. The consistent performance of the SA with the increasing number of variables suggests its ability to be scaled up while remaining competitive to the benchmark. Additionally, Table 11 shows how an increased number of potential depots, allows for a wider selection in the BSC design and, therefore, reduces investment and operation cost. The more potential depots available, the higher the likelihood the potential depot will benefit the BSC logistic distribution, such as decreasing the inefficient direct transportation of biomass to power plant (T3). The results shown in Tables 11 and 12 represent the average values from 5 runs of the SA algorithm.

As displayed in Table 12, the implementation of the SA algorithm in this two-stage stochastic model is able to outperform Bender's Decomposition when a large number of stochastic scenarios are present. However, metaheuristics reach solutions through random processes and need to be tested in order to assess their reliability. Therefore, the SA algorithm was tested to ensure its consistency and determine its drawbacks as a nondeterministic solution. Refer to Fig. 8, where the same instance, ID 5, was solved 20 times using the SA. It is noteworthy that the solutions presented in Table 12 show the average of the runs and not the overall BS of the runs. The average BS from the runs in Table 12 is reported in order to avoid any extremes in the performance metrics of the SA. For ID 5, the BS encompassing all of the runs is shown in Fig. 8 as well as the deviation compared to the average (seen in Table 12). It reached a near equal response with less than 2% of a standard deviation and a time reduction of 97.46%. It is noteworthy in Fig. 8 that the SA algorithm was able to obtain a solution on the first few iterations and remain constant, meaning that no other neighborhood moves were able to further reduce the investment cost.

7. Conclusions

In this study, we introduce a two-stage hub-and-spoke stochastic model for co-firing BSC design in combination with the development and application of a hybrid SA metaheuristic solution procedure, which was applied to a realistic case study considering yield uncertainty under various weather conditions and biomass quality variability, including moisture and ash. In doing so, we extend the works seen in the literature via the presented model and methodology mentioned as an applied to a realistic BSC design. Weather models from multiple agencies were implemented to determine yield uncertainty in multiple stochastic scenarios, and biomass quality variability was determined using INL biomass experimental samples for realistic ratios of ash and moisture. Additionally, we proposed a SA-based solution procedure, which provided good quality solutions in comparison to Bender's Decomposition benchmark method: The overall investment was less than 7.71% when comparing the average best solution of the SA with respect to the best solution of Bender's Decomposition. Additionally, the metaheuristic solution procedure allowed for large scale problems to be solved without the obstruction of memory present in the BD methods, with an average time difference of 91.4%. The proposed model and its associated solution procedure could aid decision-makers in the design of biomass supply chains considering multiple future yield scenarios.

8. Future work

These promising results open up new possibilities for future research in the area of metaheuristics implementation for the design of large-scale BSCs. By developing alternative solution procedures to computationally heavy problems, we are able to increase complexity further such as extending the model to a multicriteria optimization model. Such as additionally minimizing land usage and/or emissions in order to further reduce the impact of the BSC. Additional algorithmic development is also necessary to create and test metaheuristics as alternative solution procedures to improve search accuracy and overall solution.

CRediT authorship contribution statement

Maria Aranguren: Conceptualization, Methodology, Writing – original draft. **Krystel K. Castillo-Villar:** Conceptualization, Funding acquisition, Project administration, Supervision, Writing – review & editing. **Mario Aboytes-Ojeda:** Conceptualization, Methodology.

Declaration of competing interest

The authors declare that they have no known competing financial interests or personal relationships that could have appeared to influence the work reported in this paper.

Acknowledgments

This material is based upon work that is supported by the National Institute of Food and Agriculture (NIFA), U.S. Department of Agriculture (USDA), under the Hispanic Serving Institutions Education Grants Program, award no. 2020-38422-32258.

The authors acknowledge Dr. Marcio Giacomoni for his guidance on the data collection of climate projections, the World Climate Research Programme's Working Group on Coupled Modelling, and the climate modeling groups (listed in Table 7 of this paper) for producing and making available their model output.

References

Aboytes-Ojeda, M., Castillo-Villar, K.K., Eksioglu, S.D., 2019. Modeling and optimization of biomass quality variability for decision support systems in biomass supply chains. Ann. Oper. Res. http://dx.doi.org/10.1007/s10479-019-03477-8.

Aboytes-Ojeda, M., Castillo-Villar, K.K., Roni, M.S., 2020. A decomposition approach based on meta-heuristics and exact methods for solving a two-stage stochastic biofuel hub-and-spoke network problem. J. Cleaner Prod. 247, 119176. http://dx.doi.org/10.1016/j.jclepro.2019.119176.

Aguilar, F.X., Goerndt, M.E., Song, N., Shifley, S., 2012. Internal, external and location factors influencing cofiring of biomass with coal in the U.S. northern region. Energy Econ. 34, 1790–1798. http://dx.doi.org/10.1016/j.eneco.2012.07.005.

Anon, 2017. National land cover database (NLCD);, multi-resolution land characteristics consortium (MRLC). URL https://www.mrlc.gov/.

Aranguren, M., Castillo-Villar, K., Aboytes-Ojeda, M., Giacomoni, M., 2018. Simulation-optimization approach for the logistics network design of biomass co-firing with coal at power plants. Sustainability 10, 4299. http://dx.doi.org/10.3390/su10114299, URL http://www.mdpi.com/2071-1050/10/11/4299.

Ba, B.H., Prins, C., Prodhon, C., 2016. Models for optimization and performance evaluation of biomass supply chains: An Operations Research perspective. Renew. Energy 87, 977–989. http://dx.doi.org/10.1016/j.renene.2015.07.045.

Daioglou, V., Doelman, J.C., Wicke, B., Faaij, A., van Vuuren, D.P., 2019. Integrated assessment of biomass supply and demand in climate change mitigation scenarios. Global Environ. Change 54, 88–101. http://dx.doi.org/10.1016/j.gloenvcha.2018.11.012.

Eiselt, H.A., Marianov, V., 2009. A conditional p-hub location problem with attraction functions. Comput. Oper. Res. 36, 3128–3135. http://dx.doi.org/10.1016/j.cor.2008.11.014.

esri, 2020. ArcGIS desktop ArcMap. URL https://desktop.arcgis.com/en/arcmap/.

Ghaderi, H., Pishvaee, M.S., Moini, A., 2016. Biomass supply chain network design : An optimization-oriented review and analysis Biomass supply chain network design : An optimization-oriented review and analysis. Ind. Crops Prod. 94, 972–1000. http://dx.doi.org/10.1016/j.indcrop.2016.09.027.

Griffith, A.P., Epplin, F.M., Redfearn, D.D., 2010. Cost of Producing Switchgrass for Biomass Feedstock. Departments of Agricultural Economics and Plant and Soil Sciences, Oklahoma State University, Stillwater.

Hart, J., Castillo, K., Kiniry, J., 2016. Biomass Supply Chain Logistics for Co-Firing Coal Power Plants. ProQuest Dissertations Publishing (Ph.D. thesis). University of Texas at San Antonio, San Antonio, Retrieved from URL http://search.proquest.com/docview/1793669181/.

Idaho National Lab, 2019. Bioenergy feedstock library. URL https://bioenergylibrary.inl.gov/Sample/SampleSearchGlobal.aspx.

Jaap, K., Sjaak, V.L., 2008. The Handbook of Biomass Combustion and Cofiring. Earthscan, London, Sterling, VA.

Kenney, K.L., Smith, W.A., Gresham, G.L., Westover, T.L., 2013. Understanding biomass feedstock variability. Biofuels 4, 111–127. http://dx.doi.org/10.4155/bfs.12.83.

Kiniry, J.R., Sanderson, M.A., Williams, J.R., Tischler, C.R., Hussey, M.A., Ocumpaugh, W.R., Read, J.C., Esbroeck, G.V., Reed, R.L., 1996. Simulation alamo switchgrass with the ALMANAC model. Agron. J. 88, URL https://www.ars.usda.gov/ARSUserFiles/30980000/almanac/SimulatingAlamo.pdf.

Kizha, A.R., Han, H.S., Montgomery, T., Hohl, A., 2015. Biomass power plant feedstock procurement: Modeling transportation cost zones and the potential for competition. Calif. Agric. 69, 184–190. http://dx.doi.org/10.3733/ca.v069n03p184.

Laporte, A.V.D., Weersink, A.J., McKenney, D.W., 2016. Effects of supply chain structure and biomass prices on bioenergy feedstock supply. Appl. Energy 183, 1053–1064. http://dx.doi.org/10.1016/j.apenergy.2016.09.049.

Larson, J.A., Yu, T., English, B.C., Mooney, D.F., Wang, C., 2010. Cost evaluation of alternative switchgrass producing, harvesting, storing, and transporting systems and their logistics in the Southeastern USA. Agric. Finance Rev. 70, 184–200. http://dx.doi.org/10.1108/00021461011064950, URL http://www.emeraldinsight.com/doi/10.1108/00021461011064950.

Lautala, P.T., Hilliard, M.R., Webb, E., Busch, I., Richar Hess, J., Roni, M.S., Hilbert, J., Handler, R.M., Bittencourt, R., Valente, A., Laitinen, T., 2015. Opportunities and challenges in the design and analysis of biomass supply chains. Environ. Manag. 56, 1397–1415. http://dx.doi.org/10.1007/s00267-015-0565-2.

Liu, Z., Johnson, T.G., Altman, I., 2016. The moderating role of biomass availability in biopower co-firing — A sensitivity analysis. J. Cleaner Prod. 135, 523–532. http://dx.doi.org/10.1016/j.jclepro.2016.06.101.

Mirkouei, A., Haapala, K.R., Sessions, J., Murthy, G.S., 2017. A mixed biomass-based energy supply chain for enhancing economic and environmental sustainability benefits: A multi-criteria decision making framework. Appl. Energy 206, 1088–1101. http://dx.doi.org/10.1016/j.apenergy.2017.09.001.

Nur, F., Aboytes-Ojeda, M., Castillo-Villar, K.K., Marufuzzaman, M., 2020. A two-stage stochastic programming model for biofuel supply chain network design with biomass quality implications. IISE Trans. 1–24. http://dx.doi.org/10.1080/24725854.2020.1751347.

OSRM, 2017. Open source routing machine (OSRM). URL http://project-osrm.org/.

Poudel, S.R., Marufuzzaman, M., Bian, L., 2016. A hybrid decomposition algorithm for designing a multi-modal transportation network under biomass supply uncertainty. Transp. Res. E 94, 1–25. http://dx.doi.org/10.1016/j.tre.2016.07.004.

Reclamation, 2013. Downscaled CMIP3 and CMIP5 Climate and Hydrology Projections: Release of Downscaled CMIP5 Climate Projections, Comparison with Preceding Information, and Summary of User Needs. U.S. Department of the Interior, ed, Bureou of Reclation, Technical Services Center, Denver, CO.

Roni, M.S., Eksioglu, S.D., Searcy, E., Jha, K., 2014. A supply chain network design model for biomass co-firing in coal-fired power plants. Transp. Res. E 61, 115–134. http://dx.doi.org/10.1016/j.tre.2013.10.007.

Siarry, P., 2016. Metaheuristics. Springer International Publishing Switzerland.

Tillman, D.A., 2000. Cofiring benefits for coal and biomass. Biomass Bioenergy 19, 363–364. http://dx.doi.org/10.1016/S0961-9534(00)00048-9.

U.S. Department of Agriculture, 2017. Land values and cash rents.

U.S. Department of Agriculture Web Soil Survey, 2017. SSURGO. URL https://websoilsurvey.sc.egov.usda.gov/App/WebSoilSurvey.aspx.

U.S. Department of Energy, 2016. 2016 Billion-Ton Report: Advancing Domestic Resources for a Thriving Bioeconomy, Volume 1: Economic Availability of Feedstocks, Vol. 1160. ORNL/TM-2016/160, Oak Ridge National Laboratory, p. 448, URL http://energy.gov/eere/bioenergy/2016-billion-ton-report. doi:ORNL/TM-2016/160,

U.S. Energy Information Administration, 2017. Electricity in the United States.

U.S. Environmental Protection Agency, 2016. Emissions & generation resource integrated database (eGRID).

van Vuuren, D.P., Edmonds, J., Kainuma, M., Riahi, K., Thomson, A., Hibbard, K., Hurtt, G.C., Kram, T., Krey, V., Lamarque, J.F., Masui, T., Meinshausen, M., Nakicenovic, N., Smith, S.J., Rose, S.K., 2011. The representative concentration pathways: An overview. Clim. Change 109, 5–31. http://dx.doi.org/10.1007/s10584-011-0148-z.

Zand Atashbar, N., Labadie, N., Prins, C., 2018. Modelling and optimisation of biomass supply chains: a review. Int. J. Prod. Res. 56, 3482–3506. http://dx.doi.org/10.1080/00207543.2017.1343506.